12-2014

The search for Bose-Einstein condensation of excitons in Cu2O: exciton-Auger recombination versus biexciton formation

James P. Wolfe

Joon I. Jang
Binghamton University--SUNY

The search for Bose–Einstein condensation of excitons in Cu_2O: exciton-Auger recombination versus biexciton formation

New Journal of Physics
The open access journal at the forefront of physics
Deutsche Physikalische Gesellschaft DPG | IOP Institute of Physics

The search for Bose–Einstein condensation of excitons in Cu_2O: exciton-Auger recombination versus biexciton formation

James P Wolfe[1] **and Joon I Jang**[2]

[1] Physics Department and Materials Research Laboratory, University of Illinois at Urbana-Champaign, 1110 West Green Street, Urbana, Illinois 61801, USA
[2] Department of Physics, Applied Physics and Astronomy, State University of New York (SUNY) at Binghamton, P.O. Box 6000, Binghamton, New York 13902, USA
E-mail: j-wolfe@illinois.edu

Received 11 June 2014, revised 15 October 2014
Accepted for publication 10 November 2014
Published 17 December 2014

New Journal of Physics **16** (2014) 123048

doi:10.1088/1367-2630/16/12/123048

Abstract

Excitons in high-purity crystals of Cu_2O undergo a density-dependent lifetime that opposes Bose–Einstein condensation (BEC). This rapid decay rate of excitons at a density n has generally been attributed to Auger recombination having the form $dn/dt = -An^2$, where A is an exciton-Auger constant. Various measurements of A, however, have reported values that are orders-of-magnitude larger than the existing theory. In response to this conundrum, recent work has suggested that excitons bind into excitonic molecules, or biexcitons, which are short-lived and expected to be optically inactive. Of particular interest is the case of excitons confined to a parabolic strain well—a method that has recently achieved exciton densities approaching BEC. In this paper we report time- and space-resolved luminescence data that supports the existence of short-lived biexcitons in a strain well, implying an exciton loss rate of the form $dn/dt = -2\,Cn^2$ with a biexciton capture coefficient $C(T)$ proportional to $1/T$, as predicted by basic thermodynamics. This alternate theory will be considered in relation to recent experiments on the subject.

Keywords: exciton, biexciton, Bose–Einstein condensation, two-body recombination, cuprous oxide

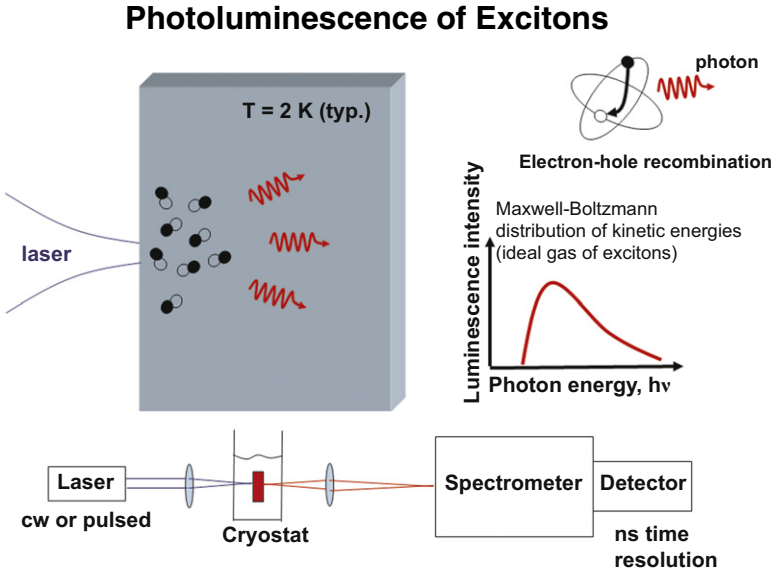

Figure 1. Summary of a photoluminesce experiment showing a basic experimental setup and schematic of a low-power luminescence spectrum in the classical-statistics regime.

1. Introduction

Cuprous oxide (Cu_2O) is a thoroughly studied direct-gap semiconductor with long-lived, highly mobile excitons [1][3]. A yellow-band exciton in this semiconductor is the positronium-like bound state of an electron and a hole with a dipole-forbidden gap of 2.173 eV. The 1s exciton exhibits an unusually strong binding energy E_x = 153 meV due to the relatively large electron and hole effective masses under dielectric screening. Considering electron and hole spin, the low-lying 1s configuration in Cu_2O is split by the electron–hole exchange interaction, producing triply-degenerate orthoexcitons and non-degenerate paraexcitons [2][4]. The ortho-para splitting energy Δ equals 12 meV under no external perturbation, with para lying lowest. The triple degeneracy of orthoexcitons can be removed under external stress [3] or magnetic field [4]. A common means of detecting excitons is photoluminescence, as illustrated in figure 1.

In high-purity crystals, long exciton lifetimes and no spectroscopic evidence for excitonic molecules suggested that the excitons are good candidates for Bose–Einstein Condensation (BEC)[5]. Early time-resolved luminescence experiments [6, 7] on high-purity Cu_2O seemed to support this idea, but a strong exciton decay process was found to limit their densities to well below the critical density for condensation. The effect was attributed to an Auger process, whereby inelastic scattering of two excitons results in recombination of one exciton and ionization of the other, producing a hot electron–hole (e–h) pair which thermalizes into a single exciton. Imagine creating excitons with a short pulse and watching the exciton density decay

[3] Drift mobilities of excitons in high purity Cu_2O are 10^7 cm^2 eV^{-1} s^{-1} at 1.2 K, corresponding to diffusivities of 1000 cm^2 s^{-1}, measured by [1].

[4] For theoretical reviews of the spectroscopic properties of forbidden-gap semiconductors, see [2].

[5] BEC of excitons was initially proposed by Blatt *et al* [5] and reviewed by Moskalenko *et al*.

due to Auger events. A simplified rate equation for the exciton density $n(t)$ is given by,

$$\frac{\mathrm{d}n}{\mathrm{d}t} = -\frac{n}{\tau} - An^2, \tag{1}$$

where $n \equiv n_{\mathrm{ortho}} + n_{\mathrm{para}}$, τ is the impurity-limited lifetime, and A is the Auger constant for excitons. The n-squared term comes about because the collisional rate for a *particular* exciton is proportional to n, and for a gas of n excitons the collisional rate goes like n^2. Classically one expects that $A = \sigma v$ with σ a constant hard-sphere cross section and v the average particle velocity proportional to $T^{1/2}$. The quantum-mechanical calculation is not so simple, but in the high-temperature limit both *direct* and *phonon-assisted* Auger processes are predicted to have $A(T) \propto T$, as discussed below.

2. Measurements of exciton dynamics in stress-free high-purity crystals: a case for excitonic molecules

A common method for producing high densities of excitons is pulsed laser excitation with photon energies larger than the Cu_2O bandgap. E–h pairs are created near the crystal surface and quickly bind into excitons which diffuse away from the excitation area. The density and temperature of the excitonic gas decrease with distance from the excitation surface. To deal with the rapidly changing gas, methods were developed to calibrate and time-resolve (1) the *total number of excitons in the gas N*, (2) the *average gas temperature T* and (3) an *effective gas volume V*. For a *thermalized* gas of ortho and paraexcitons at a crystal temperature of 70 K, an Auger constant of $A = 0.7 \times 10^{-16}\,\mathrm{cm}^3\,\mathrm{ns}^{-1}$ was obtained from the time decay of orthoexciton luminescence [8], (Orthos have 500 times the radiative efficiency of paras in high quality unstressed crystals.) Similar values for A were measured at a crystal temperature of 2 K; however, in those cases the exciton gas at nanosecond measurement times was not in thermal equilibrium with the crystal lattice [9] [6].

For a crystal temperature of 2 K, a detailed analysis of the gas dynamics following a 10 ns laser pulse found that the maximum exciton densities were about 100 times lower than the predicted critical density for BEC [10]. The time-resolved luminescence spectrum in figure 2(a) shows the kinetic energy distribution of the exciton gas at a high density. The energy distribution (solid trace) shows a remarkable similarity to the energy distribution of an ideal gas in the quantum limit, shown as the dashed trace; however, the measured gas densities were well below the quantum regime. As a function of time, the corresponding *gas temperatures* following the short excitation pulse decreased from about 100 K to 3 K, as plotted in figure 2(b).

At a crystal temperature of 111 K, the orthoexciton spectrum and decay following a 5 ps laser pulse is shown in figure 3(a) [11]. For calibrated exciton numbers, $N(T)$, and measured gas volumes, $V(T)$, fits to similar exciton transients reveal that the Auger constant has an inverse-T dependence, consistent with the earlier determination of $0.7 \times 10^{-16}\,\mathrm{cm}^3\,\mathrm{ns}^{-1}$ at a crystal

[6] O'Hara, Suilleabhain and Wolfe's [9] figure 4 showed the inconsistency of Bose statistics by comparing 2 K and 70 K luminescence spectra at calibrated densities. O'Hara, Gullingsrud and Wolfe [9] introduced time-resolved imaging to calibrate the gas volume.

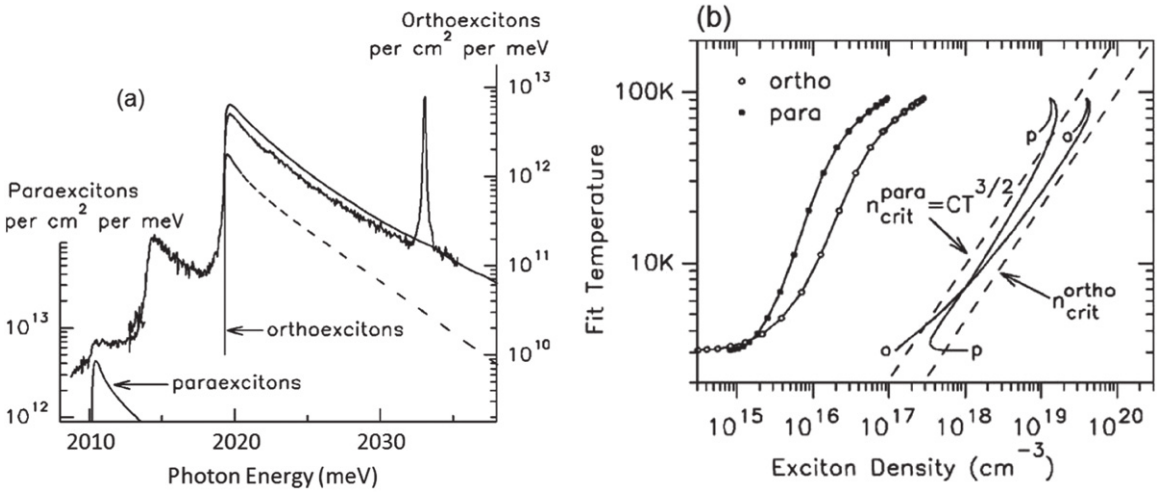

Figure 2. (a) Time-resolved luminescence spectrum used to determine the average density and temperature of the exciton gas shortly after an excitation pulse. The high-purity, unstressed crystal was immersed in liquid He at 2 K and excited with a 10 ns Ar^+ laser pulse that filled a 50 μm slit placed on its surface. The solid curve is a numerical model based on Maxwell–Boltzmann statistics and the classical diffusion of excitons. The dashed line shows a similar Bose–Einstein shape but plotted at 500-times lower density than that of a quantum gas. (b) Exciton gas temperature versus gas density from fits of luminescence spectra at times following surface excitation of Cu_2O. The measured $n(T)$ for ortho (circles) and para (dots) fall two orders-of-magnitude below the predicted BEC thresholds (dashed lines). The curves labeled *o* and *p* show gas densities derived from fitted (unphysical) quantum distributions. Reprinted with permission from [10]. Copyright 2000 American Physical Society.

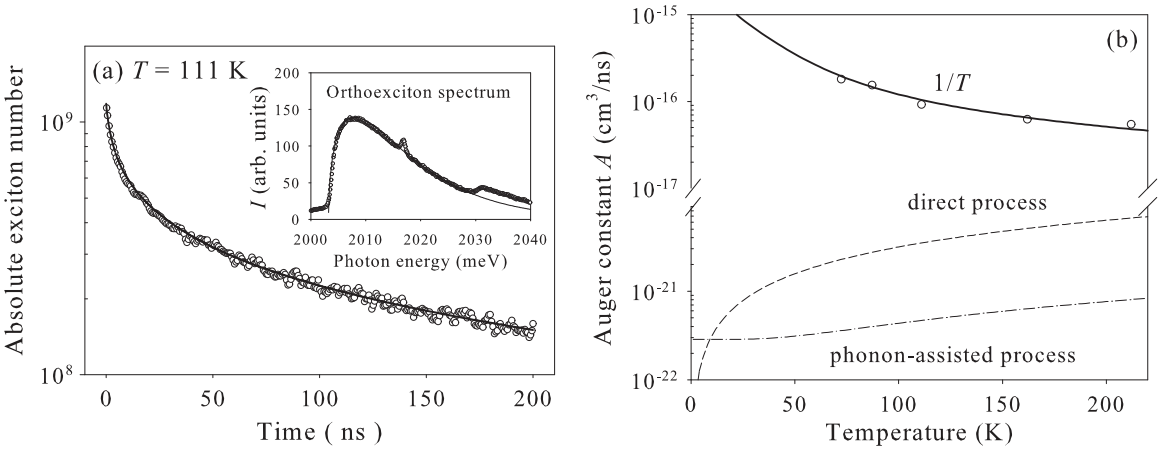

Figure 3. (a) Time decay of orthoexciton luminescence following a 5 ps laser pulse. Inset: corresponding luminescence spectrum, fit to a classical distribution at a gas temperature equal to the measured crystal temperature. (b) Measured exciton-Auger constants A from fits to equation (1) for a range of temperatures, showing a $1/T$ dependence. Dashed traces are predictions based on the theory of [12] (See footnote 7). Reprinted with permission from [11]. Copyright 2005 American Physical Society.

temperature of 70 K; see figure 3(b). In stark contrast to these measurements, a *theoretical calculation* [12] [7] of the Auger constant in Cu_2O yielded $A \simeq 3 \times 10^{-21}\,\mathrm{cm^3\,ns^{-1}}$—roughly five orders of magnitude smaller than the data. A comparison of theory and experiments is shown in figure 3(b). The weakness of the calculated Auger process stems from the same parity of the conduction and valence bands.

In view of the huge disparity between theoretical and experimental values of A, we proposed that the short lifetimes of excitons are due to their binding into short-lived biexcitons [11, 13, 14][8]. The proximity of e–h pairs in the molecule would cause a much faster Auger decay than that of two free excitons at the thermodynamic gas density. In this case, the rapid thermodynamic binding of excitons into molecules would limit the exciton lifetime, and equation (1) is replaced by the following two equations [14]

$$\frac{\mathrm{d}n}{\mathrm{d}t} = -\frac{n}{\tau} + \frac{n_b}{\tau_\mathrm{A}} - 2\,Cn^2 + 2\,Cn^* n_b, \tag{2}$$

$$\frac{\mathrm{d}n_b}{\mathrm{d}t} = -\frac{n_b}{\tau_\mathrm{A}} + Cn^2 - Cn^* n_b, \tag{3}$$

with $Cn^2 \equiv (C_\mathrm{o} n_\mathrm{o}^2 + C_\mathrm{p} n_\mathrm{p}^2)$ defining the average 'capture coefficient' for ortho and paraexcitons binding into molecules and n_b as the biexciton density. C depends on temperature, particle masses, and the binding energy of the biexciton. The symbol τ_A represents the *Auger-limited* lifetime of the biexciton. Unlike an 'exciton-Auger' event in which two colliding excitons are replaced by a single exciton, the two colliding excitons in the capture event form a single biexciton, explaining the factors of 2 in equation (2). When a biexciton undergoes Auger decay, the ejected e–h pair eventually binds into an exciton, adding to the total exciton density n via the n_b/τ_A terms above. The last terms in equations (2) and (3) represent the quasi-equilibrium thermodynamics between excitons and biexcitons. The mass-action density for this process is given by

$$n^*(T) = \frac{n^2}{n_b} = \left(\frac{mk_BT}{4\pi\hbar^2}\right)^{3/2} \mathrm{e}^{-\phi/k_BT}, \tag{4}$$

which is plotted in figure 4 for several biexciton binding energies, ϕ. Notice that an exciton density $n = n^*$ also corresponds to $n_b = n^*$.

Strictly speaking, the components of an excitonic system are not in thermal and chemical equilibrium because the excitonic matter has a finite lifetime. Equations (2)–(4) assume that a 'quasi-equilibrium' is achieved more rapidly than the overall decay time, providing an effective gas temperature and chemical potential as a function of time. The law of mass action assumed in this analysis is supported by excellent spectral fits to the time-resolved luminescence spectra during the decay process.

A detailed analysis of the exciton dynamics for a variety of experimental conditions was reported in [14]. The experiments were divided into two regimes: (1) the high-T regime

[7] To evaluate the deformation potential for phonon-assisted Auger decay, Kavovlakis and Baym [12] incorrectly used a paraexciton radiative lifetime of 14 μs. The value $3 \times 10^{-21}\,\mathrm{cm^3\,ns^{-1}}$ stated in the text follows from the correct paraexciton radiative lifetime of 7 ms, determined from measurements of Snoke and co-workers [12].

[8] In contrast to Cu_2O, a luminescence spectrum of strain-confined excitons and biexcitons was observed in high-purity Si by Gourley and Wolfe [13].

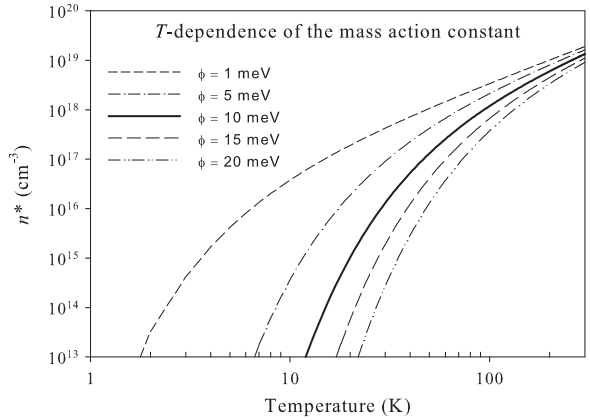

Figure 4. Temperature dependence of the mass action density $n^*(T)$ for several binding energies ϕ. Reprinted with permission from [14]. Copyright 2006 American Physical Society.

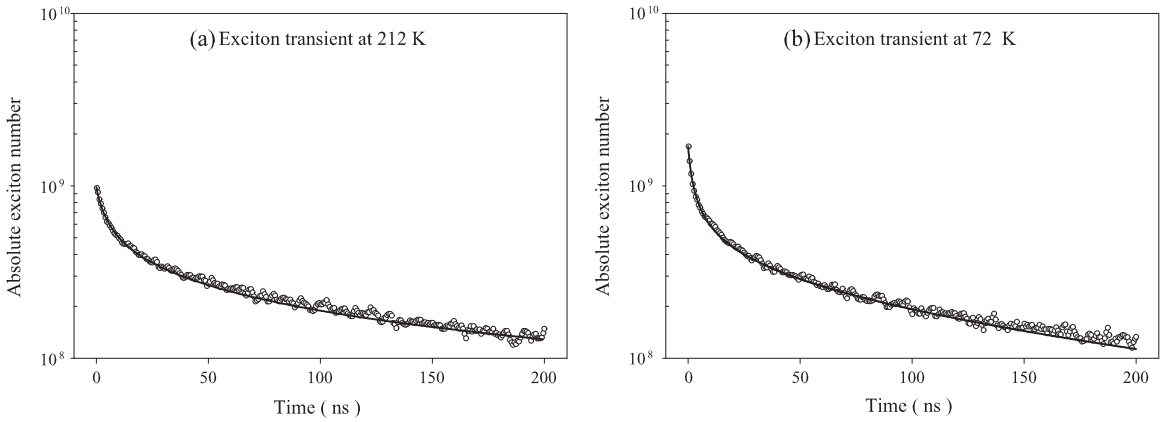

Figure 5. Measured decay transients of total exciton numbers, $N(t)$, bracketing the high-temperature range, 72–212 K. Solid curves are generated by the $N(t)$ and $N_b(t)$ rate equations for this temperature range, which incorporate the observed gas volume $V(t)$ for a given temperature. Resulting capture coefficients are given in the text. The initial rates are indicative of the $1/T$ dependence of the exciton capture coefficient, $C(T)$, as explained in the text. Reprinted with permission from [14]. Copyright 2006 American Physical Society.

($n < n^*$) where the exciton numbers dominate, and (2) the low-T regime ($n > n^*$) where biexciton numbers dominate. We emphasize that our model requires three *orthogonal* parameters $\{C, \phi, \tau_A\}$ to explain the series of exciton transients taken over a broad temperature range (2–212 K). Other density-independent relaxation rates were directly measured as detailed in [14]. Absolute exciton numbers were determined by calibration of the total luminescence intensities emitted from measured gas volumes in an unstressed crystal. Exciton transients following 5 ps pulses in the high-T regime are plotted in figure 5, showing excellent agreement with the theory of exciton/biexciton kinetics and an expected increase in the exciton decay rate at lower temperatures. The measured capture coefficients were $C(72\,\mathrm{K}) = 0.6 \times 10^{-16}\,\mathrm{cm}^3\,\mathrm{ns}^{-1}$ and $C(212\,\mathrm{K}) = 0.1 \times 10^{-16}\,\mathrm{cm}^3\,\mathrm{ns}^{-1}$. These values represent the average capture coefficient for

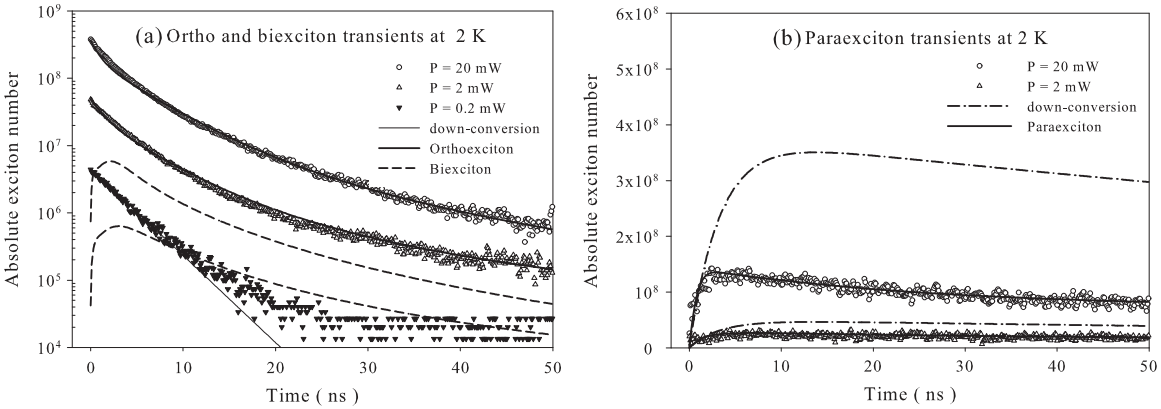

Figure 6. (a) Transients of the absolute orthoexciton number $N_o(t)$ following a 5 ps pulse, for three excitation levels. Dashed curves are the corresponding biexciton numbers derived from the experimental fits and theory. (b) Paraexciton transients $N_p(t)$. The dashed-dotted traces are predicted for no biexciton formation. The analysis for capture coefficients, C_o and C_p , incorporates direct measurements of the gas volume, $V(t)$. The analysis includes ortho-para down-conversion, needed for the short excitation pulses and ns detection. Reprinted with permission from [14]. Copyright 2006 American Physical Society.

ortho and paraexcitons, and correspond to $C_p(72\,\mathrm{K}) = 1.2 \times 10^{-16}\,\mathrm{cm^3\,ns^{-1}}$ and $C_p(212\,\mathrm{K}) = 0.4 \times 10^{-16}\,\mathrm{cm^3\,ns^{-1}}$. (Note that $C_p(72\,\mathrm{K})/C_p(212\,\mathrm{K}) = 3 \simeq (1/72\,\mathrm{K}) \div (1/212\,\mathrm{K})$.) Results for this range of temperatures are plotted in figure 3(b), with the correspondence $A \rightarrow C$.

Reference [14] examines the capture coefficients of orthoexcitons and paraexcitons more generally. With the assumption that biexcitons will be created in their para–para state either by the binding of two paraexcitons or by two orthoexcitons of opposite spin alignment, one expects $C_o = C_p/3$ and $C_{op} = 0$, which leads to an average capture coefficient C applicable to both temperature regimes and given by:

$$Cn^2 = C_o n_o^2 + C_p n_p^2 = C_p\left(n_o^2/3 + n_p^2\right). \tag{5}$$

For lattice temperatures $T_L \geqslant 50$ K, n_o/n_p only depends on T_L by a Boltzmann factor and is constant during a luminescence transient, so both C and C_p are constants. At low T_L, n_o, n_p and gas temperature T change with time making the analysis more detailed. For the temperature range 2–212 K, an overall best fit of the form $C_p(T) = c_m/T$ was found that fit all the data with about 35% variance. Specifically

$$C_p = \left[(1.4 \pm 0.4) \times 10^{-14}\right]/T\,(\mathrm{K})\ \mathrm{cm^3\,ns^{-1}}. \tag{6}$$

In particular, experiments at $T_L = 2$ K showed excellent agreement between this analysis and the experimental luminescence decays for both ortho and para excitons, as shown in figure 6.

Last but not least, both the low-T and high-T analyses require a value for the biexciton Auger rate, τ_A^{-1} and binding energy ϕ, introduced in equations (2)–(4) Reference [14] presents theoretical arguments that there is no Auger decay of biexcitons at zero kinetic energy due to band orthogonality, and at finite temperature, $\tau_A^{-1}(T) = a_m T$. This form was used in the

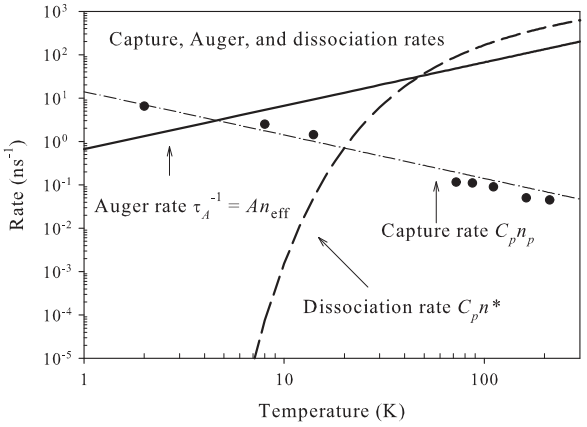

Figure 7. Temperature dependences of the para–para capture rate, biexciton dissociation rate and Auger decay rate assuming $n_{\rm p} = 10^{15}\,{\rm cm}^{-3}$ for $T = 2$–$212\,{\rm K}$. Reprinted with permission from [14]. Copyright 2006 American Physical Society.

analyses and produced best-fit values, $a_m = 0.5\,{\rm ns}^{-1}\,{\rm K}^{-1}$, and a biexciton binding energy $\phi = 10$ meV for the unstressed crystal. Figure 7 shows the temperature dependences of these fundamental rates. In [14] we considered the direct (no-phonon) Auger decay process; however, a *phonon-assisted* biexciton Auger decay would also lead to a linear temperature dependence of the Auger process.

As mentioned earlier, biexcitons with symmetry Γ_1^+ in this forbidden-gap semiconductor are expected to be optically inactive [15] and, so far, no spectroscopic evidence of their existence has been reported [16], although 2-photon spectroscopy [17, 18][9] seems a possibility. Theoretical calculations show a small but significant binding energy, of order 3–13 meV[10].

3. Strain-confinement of excitons in Cu_2O

The aforementioned complications of heating and diffusion of the exciton gas can be greatly reduced by employing a Hertzian contact stress [19]. Upon application of pressure with a rounded stress rod, a shear-stress maximum is produced inside the crystal that corresponds to a lowered bandgap—forming a parabolic trap for excitons. Strain confinement was introduced for excitonic matter in Ge and Si crystals [20] and first applied to the thermodynamics of ortho and paraexcitons in Cu_2O at crystal temperatures near 2 K [21]. Figure 8(a) is a photoluminescence image of paraexcitons confined to a strain well in Cu_2O at 2 K. In this case, a continuous Ar^+ laser beam produced excitons near the crystal surface, and a stream of long-lived paraexcitons are drawn into the trap. The principal motivation for such experiments was to create an environment for BEC of excitons, analogous to the optical confinement of atomic gases that has led to BEC and amazing new properties of quantum gases [22, 23].

Excitons can also be generated directly in the trap by using photons with energy slightly below the unstressed bandgap, as depicted in figure 8(b). Photons are transmitted through the

[9] For 2-photon excitation, see Naka and Nagasawa (2002) [17]. Exciton mass values from 2-photon excitation are discussed in Frohlich *et al* [17].

[10] Theoretical calculations of biexciton binding energies in Cu_2O are summarized in [14]. The weakness of the biexciton bond is due to the large mass ratio of e and h, combined with large exchange splitting Δ.

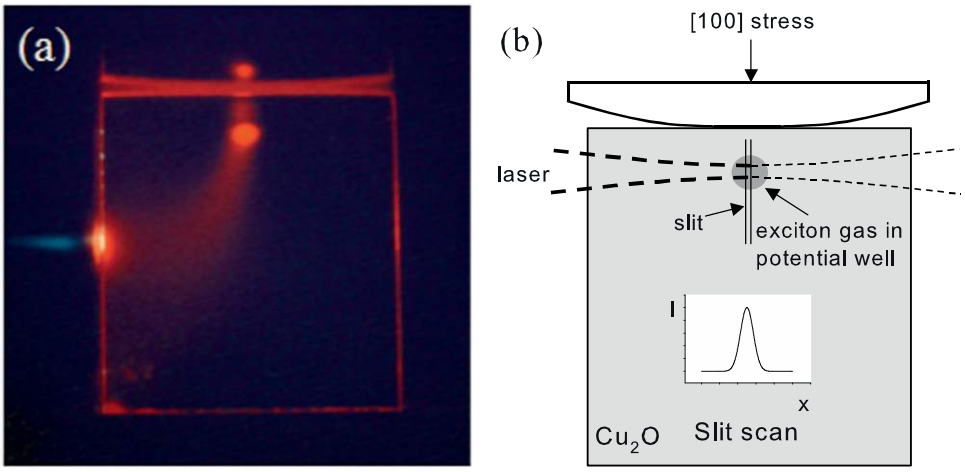

Figure 8. (a) Photoluminescence image of a pure Cu_2O crystal stressed at the top by a curved glass rod and photoexcited by a cw Ar^+ laser beam at the left surface. Excitons drift into the strain-induced potential well below the contact and are collected there. The strain-confined excitons at 2 K exhibit classical statistics, as reported in [21]. Reflections from the crystal surfaces and stressor are seen near the top of the image. Sample is a 1.5 mm cube. (b) Schematic diagram of a potential well excited directly by lower frequency light and probed by scanning the image of the crystal across a narrow slit at the entrance of a spectrometer.

low stress region and absorbed in the high stress region below the contact. The gas temperature is determined by fitting the luminescence spectrum, or by measuring the thermalized gas volume in the parabolic well, as discussed below. Near-resonant creation of orthoexcitons with pulsed excitation produces a quickly thermalized exciton gas with temperatures that approach the crystal temperature within a few nanoseconds. Calibration of the *exciton numbers*, their *temperature*, and the *gas volume* are key parameters in determining the exciton loss mechanisms. A variety of research on strain-confined excitons in Cu_2O has been reported—both experimental [17] (see footnote 9), [24–26][11] and theoretical [27, 28]. Most recently, experiments at *millikelvin* temperatures [29–32] have heightened the search for excitonic BEC, as discussed later in this paper. In the rest of this section we will describe early strain-well photoluminescence experiments that relate to the exciton-Auger versus biexciton issue. In the final two sections, remarkable millikelvin experiments with a variety of techniques will be examined with prospects for the future.

The earliest attempts to observe BEC of excitons in a strain well [21] met with the usual difficulty: shortened exciton lifetimes at high densities—initially attributed to a strong exciton-Auger process. We now re-examine in detail *the thesis data and analysis of Keith O'Hara* [33][12] in terms of our biexciton model. O'Hara employed the technique illustrated in figure 8(b). The strain well was formed by pressing a lens with radius of curvature 8.15 mm onto a (001) face of Cu_2O at 2 K, initially with a force of 340 N, producing about 1% strain in

[11] Sandfort *et al* [26] examine paraexcitons confined by a strain trap with high magnetic fields and cw pumping.
[12] The experimental data and analyses described here were reported by [33]. At that time, the large values obtained for the exciton-Auger decay were not understood, nor was the possible role of biexcitons realized. The present analysis also benefits from an accurate measurement of the ortho-para down-conversion rate, reported in [35].

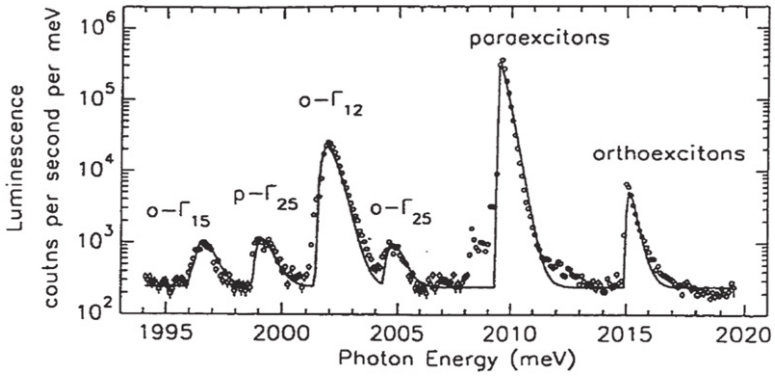

Figure 9. Luminescence spectrum at 2 K recorded 1000 ns after a 10 ns dye-laser pulse tuned 0.4 meV above the onset of the phonon-assisted orthoexciton absorption band. 10^8 photons were absorbed in the well from each pulse. Luminescence was collected along (110), perpendicular to the direction of compression. The relative intensities of the phonon-assisted luminescence lines were found to be the same as in a strain-free crystal. The spectral features are fit to the appropriate Maxwell–Boltzmann distributions and from their integrals the numbers of orthoexcitons (1×10^4) and paraexcitons (2×10^5) were determined using the calibrated luminescence intensities. From [33] (see footnote 12).

the well. Luminescence was collected along a (110) direction. Application of stress has a different effect on the spectral positions of paraexcitons and orthoexcitons: the energy splitting Δ between the lowest (doubly-degenerate) ortho state and the non-degenerate para state decreases with stress [3, 21].

Figure 9 shows a time-resolved spectrum from the strain well, recorded 1 μs after a 10 ns dye-laser pulse, pumped by a mode-locked Nd:YAG laser. The dye laser is tuned to 2028.9 meV, which is 0.4 meV above the absorption threshold for orthoexciton creation. The spectral features in figure 9 are labeled by their recombination process. For example, the $o - \Gamma_{12}^-$ line refers to orthoexciton recombination assisted by a Γ_{12}^- phonon with negative parity. The largest signal is due to direct (no-phonon) recombination of paraexcitons in the strain well —a signal that is forbidden to all orders in a *strain-free* crystal, indicating a symmetry breaking of the radiative transition under stress. The phonon-assisted paraexciton line ($p - \Gamma_{25}^-$) is weakly dipole-allowed by the negative parity of the emitted phonons, and its intensity is not significantly changed by crystal strain. At the bottom of the well, the orthoexciton onset is at $E_{\text{ortho}} = 2014.9$ meV and the paraexciton onset is at $E_{\text{para}} = 2009.3$ meV, yielding an ortho-para splitting of $\Delta = 5.6$ meV at this stress level. Most important for the determination of relative ortho and para densities, the ratio between the *radiative* rates of the Γ_{12}^- orthoexciton and the Γ_{25}^- paraexciton is known to be 500. (See, for example, [33] (see footnote 12), [34][13].)

The rate at which the photoexcited orthos convert into paras had been measured previously as a function of stress [35]. For the 5.6 meV splitting above, the measured down-conversion rate, $D \simeq 0.08\,\text{ns}^{-1}$, is four times slower than that in an unstressed sample. With this down-conversion rate the optically produced othoexcitons have decayed mainly into paraexcitons within a few nanoseconds. Considering the measured down-conversion rate, the number of

[13] Phonon-assisted transitions are explained in [34]. Chapter 3 of [33] contains a comprehensive discussion of optical absorption and luminescence in Cu_2O.

orthoexcitons at 1 μs after the excitation pulse should be reduced by a factor $e^{-D \times 1\,\mu s} = e^{-80}$. In sharp contrast, significant orthoexcitons are observed at 1 μs, as shown in figure 9. In the *exciton-Auger* model, the actual orthoexciton intensities must arise from exciton-Auger decay which produces highly excited carriers that thermalize into ortho and paraexcitons. For the *biexciton* model, ortho and paraexcitons at late time are a product of biexciton Auger decay.

For particles in a three-dimensional harmonic potential, $U(r) = \alpha r^2$, the effective volume of the gas at temperature T is $V = (2\pi k_B T/\alpha)^{3/2}$ and the average particle density is $n = N/V$, with $N = N_{\rm ortho} + N_{\rm para}$ the total number of excitons in the well. The luminescence image of the confined exciton gas was scanned parallel and perpendicular to the stress axis, as illustrated in figure 8(b), giving an effective volume, $V = (4\pi)^{3/2} \times 40 \times 50 \times 50\ \mu m^3 = (4.5 \pm 1.3) \times 10^{-6}$ cm^3.

Notice from figure 4 that at $T = 10$ K the mass-action density is roughly 10^{12} cm^{-3} and decreases exponentially at even lower temperatures. This implies that equation (2) effectively mimics equation (1) with C replacing A, because $Cn^* n_b$ terms are negligible and $n_b/\tau_{\rm A} = Cn^2$. In [33] (see footnote 12), the data was analyzed with equation (1) and a total exciton density $n = N/V$:

$$\frac{dN}{dt} = -\frac{N}{\tau} - \frac{AN^2}{V}. \tag{7}$$

For an initial exciton number N_o this equation has the solution

$$N(t) = \frac{N_o e^{-t/\tau}}{1 + (A/V)N_o\tau\left(1 - e^{-t/\tau}\right)}. \tag{8}$$

In the experiment, the spectrometer slit accepted only the central 19 μm of the exciton cloud, measuring luminescence from only 15% of the excitons in the well, plotted as the left axis in figure 10(a).

A fit of equation (8) to the measured $N(t)$ decay is shown in figure 10(b), yielding the result,

$$A(2\ {\rm K}) = 2 \times 10^{-15}\ {\rm cm^3\,ns^{-1}}, \tag{9}$$

with a factor of 2 uncertainty in the calibration of $N_{\rm o}$ from luminescence intensity. Alternatively, a value of $A = 0.5 \times 10^{-15}$ cm^3 ns^{-1} would be obtained by setting $N_{\rm o}$ equal to the number of absorbed laser photons; i.e., assuming no losses (100% quantum efficiency) in the conversion of incident photons to thermalized excitons and biexcitons. Thus, the confidence level of equation (9) is about a factor of four. O'Hara pointed out that this value of A is about *30 times larger* than the Auger constant obtained for the thermalized gas in an unstressed crystal at 70 K. Note that 70 K/2 K = 35 and that biexciton capture and its inverse-T dependence was not recognized at that time. Indeed, the measured value for 'A' in the strain-well experiment is within a factor of 4 of the capture coefficient later obtained for the unstressed crystal, (from equation (6)):

$$C_{\rm p}(2\ {\rm K}) = (7 \pm 2) \times 10^{-15}\ {\rm cm^3\,ns^{-1}}. \tag{10}$$

In an unstressed crystal, we compared a measured capture coefficient C to A_{pp} determined from an exciton-Auger analysis and reported [11]

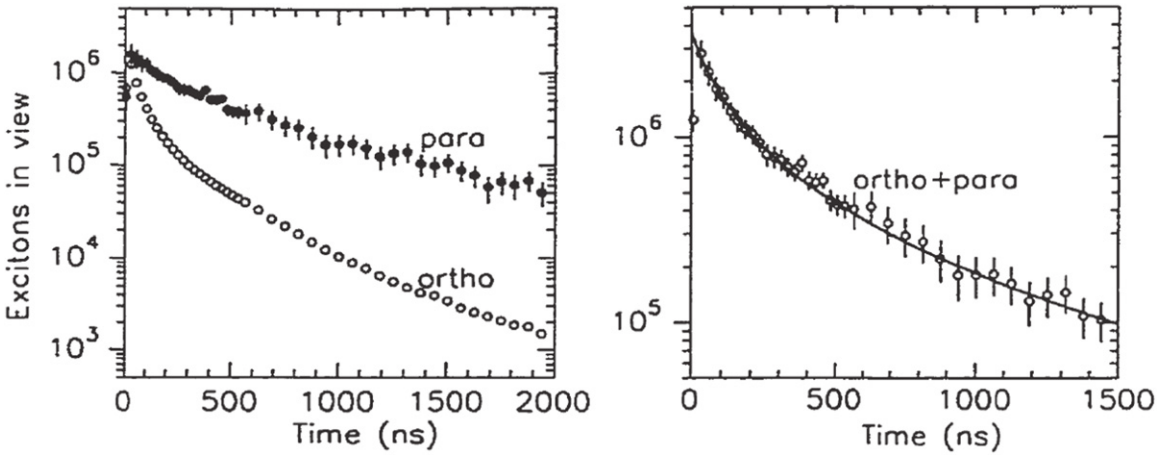

Figure 10. (a) Numbers of orthoexcitons and paraexcitons, within a 19 μm wide observation region in the strain well, following a 10 ns laser pulse containing 10^8 photons absorbed in the well at 2 K. In spite of their down-conversion time of 12.5 ns, the orthoexciton luminescence persists up to 2 μs. According to the biexciton model the orthoexcitons are a byproduct of the biexciton Auger recombination process. (b) Total number of excitons (ortho + para) in the strain well. The solid curve is a fit to equation (8), assuming 15% of the excitons in the well are monitored. The best fit parameters are $N(0) = (2.5 \pm 0.3) \times 10^7$, $C/V = 0.43 \pm 0.03\,\mathrm{s}^{-1}$, and $\tau = 1100 \pm 100$ ns. From [33] (see footnote 12).

$$C(2\ \mathrm{K}) = A_{pp} = 4 \times 10^{-15}\ \mathrm{cm}^3\ \mathrm{ns}^{-1}. \tag{11}$$

We conclude that, so far, both stressed and unstressed measurements are consistent with the biexciton theory, within experimental uncertainties. It should be noted, however, that excitation conditions were quite different for the strain-well and unstressed experiments. The unstressed work [14] used line excitation with 5 ps pulses, and the strain-well work described above employed volume excitation with 10 ns pulses. The biexciton rate equation (3) was not employed in the strain-well analysis because there were no biexciton signals to compare. A future study of the ortho and para transients in a strain-well, however, might provide information about the biexciton densities, considering that the biexciton Auger process is the only source of orthoexcitons long after a short excitation pulse. It seems possible that the biexciton Auger lifetime, τ_A, depends on stress, which would directly affect ortho and para densities and likely provide information about the biexciton wavefunction.

4. Discussion of results and relation to other work

In apparent conflict with the $1/T$ dependence of capture coefficient is a report of a nearly constant $A(T)$ over a crystal-temperature range of 5–70 K [36]. The experiments irradiated an unstressed high-purity sample with a cw dye laser set at 601 nm, producing a relatively homogeneous line of excitation along the 220 μm sample thickness. The number of paraexcitons along this line was determined from their 1s-2p induced absorption spectrum, using a mid-infrared probe beam. An advantage of this technique based on excitonic Lyman spectroscopy [37] is its ability to probe exciton numbers in the beam path over a wide range of temperatures. Remarkably, their graph of $A(T)$ reproduced in figure 11 shows

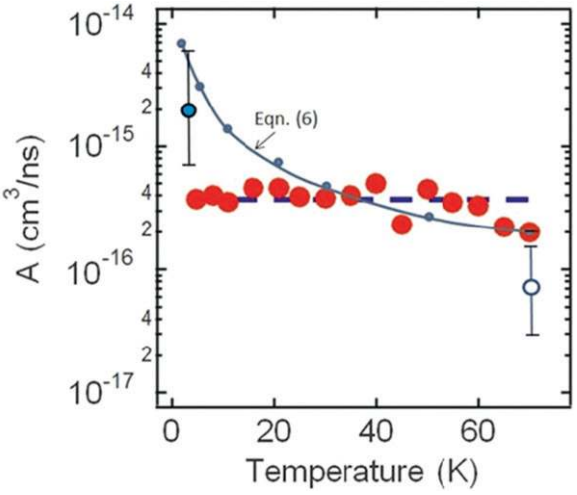

Figure 11. The large solid dots show the temperature dependence of the exciton-Auger parameter A as reported in [36] for an unstressed crystal. The curve with small dots is a plot of the biexciton capture coefficient, $C_p(T)$, given by equation (6). The filled circle at $T = 2$ K represents the strain-confined data of [33] (see footnote 12); its value and uncertainty is explained with equation (9). The open circle at 70 K is for the unstressed crystal of [8]. Theory for the exciton-Auger parameter [12] (see footnote 7) is plotted at the bottom of figure 3(b) and is five orders of magnitude below the dashed line in this figure.

$A = 2 \times 10^{-16}\,\mathrm{cm^3\,ns^{-1}}$ at a temperature of about 70 K, which is essentially the same as that predicted by the biexciton capture coefficient, $C_p(70\,\mathrm{K}) = 2 \times 10^{-16}\,\mathrm{cm^3\,ns^{-1}}$.

Figure 11 shows a direct comparison of $C_p(T)$ from equation (6) with their data. Over the temperature range 20 K–70 K the Lyman-based data is consistent with $C(T)$ from time-resolved luminescence, within a factor of 2. However, at 2 K the plotted $C_p(T)$ curve is about an order-of-magnitude higher than a constant extrapolation of the Lyman data below 5 K. A possible cause of this discrepancy is that the Lyman experiments did not directly measure the *exciton gas volume*, which is known to depend on temperature-dependent exciton diffusivities ([1], see footnote 3) and capture broadening of the gas volumes [11, 14]. In the time-resolved luminescence experiments of [14], the gas volume was obtained directly by luminescence imaging. Furthermore, the Lyman analysis was based on exciton-Auger equations, which presently have no theoretical basis.

A previous attempt at measuring $A(T)$ in the high-T regime was reported by Liu and Snoke [38], who introduced fitted parameters instead of known physical constants in the exciton-Auger theory ([12], see footnote 7). A linear-T dependence of A was obtained from time-resolved luminescence; however, for their near-surface excitation, a factor of ten variation in excitation volume over the temperature range of the measurements was not incorporated in their analysis. Including the gas volume effect would likely cause their values of A to decrease with higher T, not increase.

In quite different experiments, a claim of BEC of paraexcitons in *uniformly-stressed* Cu_2O was published by Lin and Wolfe [39]. A uniaxial (110) stress was applied to a thin crystal in order to reduce the multiplicity of the orthoexcitons from 3 to 1 at high stress levels. A *quantum-like* spectral distribution of orthoexciton energies was reported, similar to those

reported in [7]. However, in this case a narrowing of the paraexciton spectrum occurred, which was interpreted as evidence for paraexciton condensation. The origin of this striking effect remains unresolved (perhaps associated with a nonuniformity of the high stress in the thin crystal) and was not reproduced by subsequent experiments in our group [10]. Strain-confinement methods have proven to be a more reproducible method for achieving stable gas volumes of highly mobile excitons under applied stress.

Two experimental groups have succeeded in strain-confining excitons at *millikelvin temperatures* in search for BEC. Schwartz *et al* [29] have produced dense paraexcitons in a strain well at 10 K that cool in a lifetime of 500 ns to the He bath temperature of 820 mK. They present extensive luminescence data and modeling under these conditions. Most relevant here, their analysis yields exciton-Auger constants of 4.9×10^{-17} cm^3 ns^{-1} and 3.7×10^{-18} cm^3 ns^{-1} for orthoexcitons and paraexcitons, respectively—much lower than earlier reports (e.g., [36] in the strain-free case and C in the last section). Their experiments, however, utilized significantly stronger excitation conditions. Specifically, their calibrated rate-equation model indicates about 10^9 orthos and 10^{10} paras (from their figure 9) created by a 50 ns pulse, compared to 5×10^7 orthos and 4×10^7 paras at the highest levels described in the last section. In the biexciton model, gas heating would lower the capture coefficient via its $1/T$ dependence. Also, a region 100 μm away from the trap center was pumped, compared to pumping close to the trap center. Finally, a limited time resolution could have been affecting the shape of the luminescence decays. For example, the time decay of orthoexciton number in their figure 7 was collected with a relatively long 200 ns sampling time and shows a near exponential decay over four orders of magnitude, in contrast to the curved decays of ortho and paraexciton numbers commonly observed in experiments at lower excitation levels.

Yoshioka *et al* [30] have observed the behavior of strain-confined excitons at millikelvin temperatures, using a cw laser to create orthoexcitons near the center of a strain well. The orthoexcitons rapidly down-convert to paraexcitons and the gas rapidly cools via emission of acoustic phonons. The thermalized spectra and volume of the trapped gas were determined versus lattice temperature, similar to [21] but extended to sub-Kelvin temperatures. The spectral width and gas volume stopped decreasing below about 900 mK; however, at a lattice temperature of about 350 mK and strong excitation level, they observed a striking increase in the paraexciton luminescence higher in the potential well, shown in figure 12. A factor of about 3 rise in the ratio of non-thermal-to-thermal luminescence was observed when the thermal para numbers were increased from 2×10^8 to 2×10^9, which they postulated was due to an instability of Bose-condensed paraexcitons. It also seems possible that the non-thermal signal was due to Auger products from rapid biexciton decay, facilitated by efficient capture (and perhaps condensation) of biexcitons in the strain well. Promising new experiments by this group [31] have since achieved a paraexciton gas temperature of less than 100 mK (albeit at much lower gas densities), as shown in figure 13 and made possible by a stress-induced cooling of the excitons via their coupling with the low-velocity TA phonons[14].

New experiments by Stolz *et al* [32], have claimed strong evidence for BEC of excitons at millikelvin temperatures based mainly on the *spatial distributions* of *direct* paraexciton

[14] For a bath temperature of 1.2 K, Trauernicht *et al* [21] observed a significant heating of the paraexciton gas with pulsed-laser excitation. Yoshioka *et al* [31], recognized that, in addition to lower lattice temperatures, moderate (cw) excitation can be a more effective way of approaching the condensation condition. The challenge is to raise the gas density without a significant rise in gas temperature.

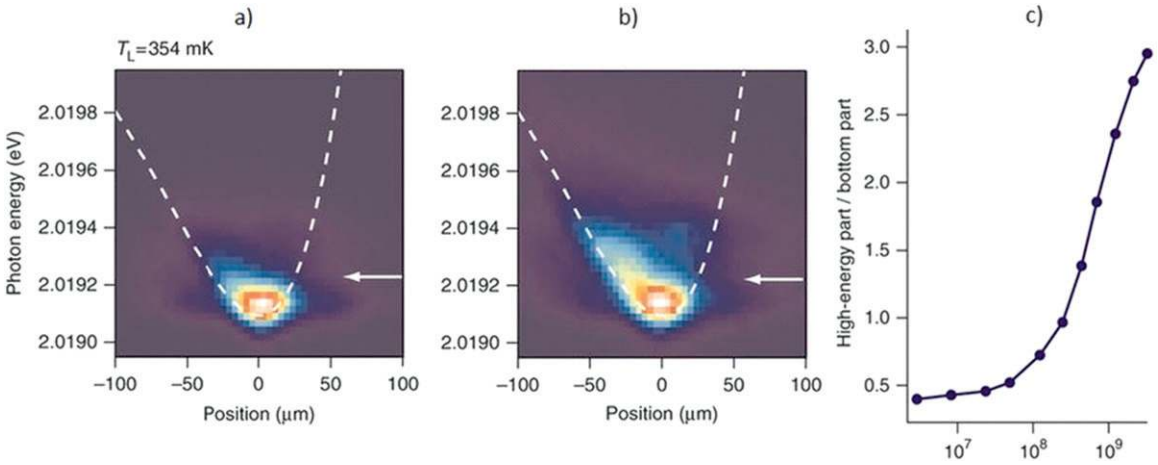

Figure 12. (a) Luminescence image of the gas of paraexcitons in a strain well at millikelvin temperature. (b) With increased excitation level there is an increase in paraexciton luminescence at higher energies in the well. (c) The ratio of intensities from the high part to the low part increases with excitation level, as plotted in the graph and interpreted as evidence for an 'explosive' condensation of paraexcitons in the bottom of the well, as discussed in [30]. Reprinted with permission from [30]. Copyright 2011 Nature Publishing Group.

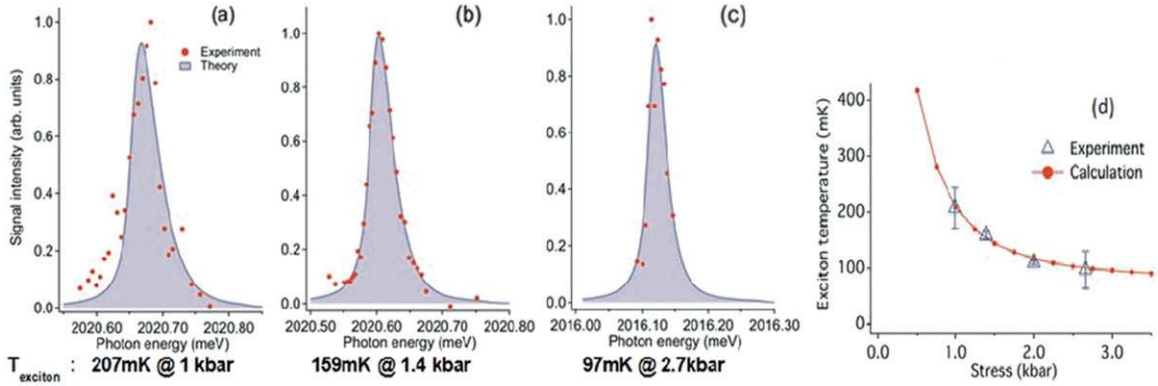

Figure 13. (a)–(c) Luminescence spectra of paraexcitons confined to a strain well at a crystal temperature of 40 mK and increasing stress level. The spectral widths are compared to theoretical distributions (shaded) to obtain the gas temperatures listed below the spectra and plotted in part. (d) Reprinted with permission from author [31]. Copyright 2013 American Physical Society.

luminescence in a strain well. The principal finding of their extensive quantitative study is highlighted in figure 14, which shows two luminescence images of the exciton gas at increasing excitation power, which raises the gas temperature. The lower-T cloud contains fewer excitons and is slightly blue-shifted compared to the extended cloud at higher T. They conclude that the 'missing excitons' from the smaller cloud (and other small clouds at lower T) are condensed excitons, which de-condense at higher T.

Naturally we ask how biexcitons impact the experimental conditions and conclusions of those experiments. Our work implies that biexcitons are the dominant particles at millikelvin

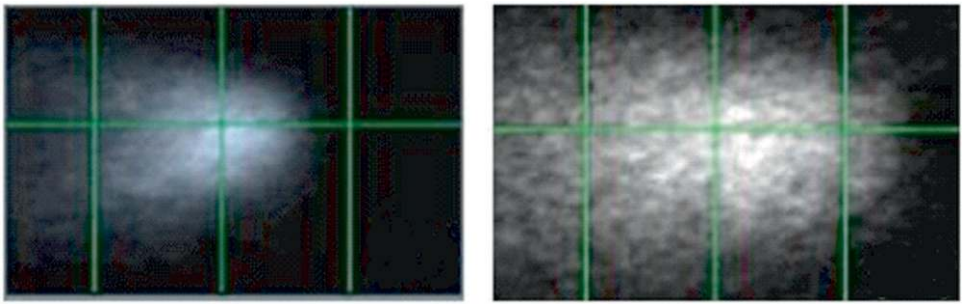

Figure 14. Changes in the spatial extent and total number of paraexcitons in a potential well as the excitation power is increased between direct-luminescence images, (a) and (b) as reported in [32]. The interpretation, based on this data and more extensive measurements, is that the 'missing excitons' in image (a) are evidence for an invisible Bose condensate, which dissipates into free excitons at the higher temperature of image (b).

temperatures based on (1) the exciton-biexciton equilibration condition and (2) the biexciton Auger lifetime which increases as $1/T$. Biexcitons (condensed or not) would also dissipate at higher temperatures. In general, one must consider the effect of these 'heavier' species on the spatial extent of the excitonic gas in a strain well. Regarding the 'invisibility' of Bose-condensed species, we suggest spatial measurements of *phonon-assisted* luminescence, as introduced in the spectroscopy experiments of [39] at near-uniform stress.

5. Summary and prospects

In an unstressed high-purity crystal of Cu_2O, calibrated measurements of orthoexciton and paraexciton densities following 5 ps excitation pulses are well explained by the biexciton formation model for crystal temperatures between 2 and 200 K. The temperature-dependent biexciton capture coefficient C measured for a stress-free crystal is consistent with that for excitons in a stress-induced trap at $T_L = 2$ K. Comparing to earlier measurements of the density-dependent recombination at 70 K, the measured value of C at $T_{\rm gas} = 2.5$ K is consistent with $C \propto T_{\rm gas}^{-1}$ and also consistent with the analysis of [11, 14] conducted at a lattice temperature of 2 K. Although a stable biexciton is optically inactive under no perturbation, the biexciton luminescence is expected to be slightly allowed under external stress. For our experimental stress level and the predicted biexciton binding energy of about 10 meV, a weak biexciton luminescence line below the direct paraexciton luminescence would have been strongly masked by the Γ_{12}^{-} orthoexciton phonon replica (see figure 9). Note that external perturbation such as electric or magnetic field is not particularly helpful because of essentially the same luminescence screening effect. Presumably, resonant 2-photon excitation tuned to $\phi/2 \sim 5$ meV below the paraexciton line could be a more viable method to probe the biexciton state under external stress in which the optical transition is weakly allowed via level mixing. Despite the present dearth of spectroscopic evidence, the large increase in exciton decay rates at low temperature strongly supports biexciton formation and decay, rather than exciton-Auger decay, for which there is presently no viable theory.

Acknowledgments

We are especially grateful to our co-workers in the search for Bose–Einstein condensation of excitons over the years. Key advances include PhD works of Paul Gourley, David Trauernicht, David Snoke, George Kavoulakis, Jia Ling Lin, and Keith O'Hara. Colleague Andre Mysyrowicz provided the impetus and initial crystals in the mid-1980s. Funding for our research was provided primarily through the Materials Research Laboratory at the University of Illinois and by the National Science foundation, as indicated in referenced publications.

References

[1] Trauernicht D P and Wolfe J P 1986 *Phys. Rev.* B **33** 8506
[2] Agekyan V T 1977 *Phys. Status Solidi* A **43** 11
Elliot R J 1957 *Phys. Rev.* **108** 1384
[3] Waters R G, Pollack F H, Bruce R H and Cummins H Z 1980 *Phys. Rev.* B **21** 1665
[4] Höger von Högersthal G B, Dasbach G, Fröhlich D, Kulka M, Stolz H and Bayer M 2005 *J. Lumin.* **112** 25
[5] Blatt J M, Böer K W and Brandt W 1962 *Phys. Rev.* **126** 1691
Moskalenko S A and Snoke D W 2000 *Bose Einstein Condensation of Excitons and Biexcitons* (Cambridge: Cambridge University Press)
[6] Hulin D, Mysyrowicz A and Benoît á la Guillaume C 1970 *Phys. Rev. Lett.* **45** 1970
[7] Snoke D, Wolfe J P and Mysyrowicz A 1990 *Phys. Rev.* B **41** 11171
Snoke D, Wolfe J P and Mysyrowicz A 1990 *Phys. Rev.* B **44** 12109 (Bose statistics suggested by spectra)
[8] Warren J T, O'Hara K E and Wolfe J P 2000 *Phys. Rev.* B **61** 8215
[9] O'Hara K E, Ó Súilleabháin L and Wolfe J P 1999 *Phys. Rev.* B **60** 10565
O'Hara K E, Gullingsrud J R and Wolfe J P 1999 *Phys. Rev.* B **60** 10872
[10] O'Hara K E and Wolfe J P 2000 *Phys. Rev.* B **62** 12909
[11] Jang J I and Wolfe J P 2005 *Phys. Rev.* B **72** 241201(R)
Jang J I and Wolfe J P 2006 *Solid State Commun.* **137** 91
[12] Kavoulakis G M and Baym G 1996 *Phys. Rev.* B **54** 16625
Snoke D W, Braun D and Cardona M 1991 *Phys. Rev.* B **44** 2991
[13] Gourley P L and Wolfe J P 1979 *Phys. Rev.* B **20** 3319
Gourley P L and Wolfe J P 1978 *Phys. Rev. Lett.* **40** 526
[14] Jang J I and Wolfe J P 2006 *Phys. Rev.* B **74** 045211
[15] Roslyak O, Aparajita U, Birman J L and Mukamel S 2012 *Phys. Status Solidi* B **249** 435
[16] Petroff Y, Yu P Y and Shen Y R 1972 *Phys. Rev. Lett.* **23** 1558
[17] Naka N and Nagasawa N 2002 *Phys. Rev.* B **65** 245203
Naka N and Nagasawa N 2004 *Phys. Rev.* B **70** 155205
Naka N and Nagasawa N 2003 *Solid State Commun.* **126** 523
Fröhlich D, Brandt J, Standfort C, Bayer M and Stolz H 2011 *Phys. Rev.* B **84** 193205 exciton mass values from 2-photon excitation
[18] Jang J I, Ketterson J B, Anderson M A and Chang R P H 2007 *Phys. Rev.* B **76** 233201
Jang J I, Sun Y and Ketterson J B 2008 *Phys. Rev.* B **77** 075201
[19] Hertz H 1881 *J. Math. (Crelles J.)* **92** 156
[20] Wolfe J P and Jeffries C D 1983 *Modern Problems in Condensed Matter Science* vol 6 ed V M Agranovich and A A Maradudin (Amsterdam: North-Holland) ch 5
[21] Trauernicht D P, Wolfe J P and Mysyrowicz A 1986 *Phys. Rev.* B **34** 2561
[22] Anderson M H, Ensher J R, Matthews M R, Weiman C E and Cornell E A 1995 *Science* **269** 198

[23] Davis K B, Mewes M-O, Andrews M R, van Druten N J, Durfee D S, Kurn D M and Ketterle W 1995 *Phys. Rev. Lett.* **75** 3969
[24] Snoke D W and Negoita V 2000 *Phys. Rev.* B **61** 2904
[25] Denev S and Snoke D W 2002 *Phys. Rev.* B **65** 085211
[26] Sandfort C, Brandt J, Finke C, Fröhlich D, Bayer M, Stolz H and Naka N 2011 *Phys. Rev.* B **84** 165215
[27] Stolz H and Semkat D 2010 *Phys. Rev.* B **81** 081302R
[28] Sobkowiak S, Semkat D, Stolz H, Koch Th and Fehske H 2010 *Phys. Rev.* B **82** 064505
[29] Schwartz R, Naka N, Kieseling F and Stolz H 2012 *New J. Phys.* **14** 023054
[30] Yoshioka K, Chae E and Kuwata-Gonokami M 2011 *Nat. Commun.* **2** 328
Yoshioka K and Kuwata-Gonokami M 2012 *New J. Phys.* **14** 055024
[31] Yoshioka K, Morita Y, Fukuoka K and Kuwata-Gonokami M 2013 *Phys. Rev.* B **88** 041201(R)
[32] Stolz H, Schwartz R, Kieseling F, Som S, Kaupsch M, Sobkowiak S, Semkat D, Naka N, Koch Th and Fehske H 2012 *New J. Phys.* **14** 105007
[33] O'Hara K E 1999 Relaxation kinetics of excitons in cuprous oxide *PhD Thesis* University of Illinois
[34] Bloch P D and Schwab C 1978 *Phys. Rev. Lett.* **41** 514
[35] Jang J I, O'Hara K E and Wolfe J P 2004 *Phys. Rev.* B **70** 195205
Jang J I and Wolfe J P 2006 *Phys. Rev.* B **73** 075207
[36] Yoshioka K, Ideguchi T, Mysyrowicz A and Kuwata-Gonokami M 2010 *Phys. Rev.* B **82** 041201R
[37] Tayagaki T, Mysyrowicz A and Kuwata-Gonokami M 2006 *Phys. Rev.* B **74** 245127
[38] Liu Y and Snoke D 2006 *Solid State Commun.* **140** 208
[39] Lin J L and Wolfe J P 1993 *Phys. Rev. Lett.* **71** 1222